

# Development and evaluation of small loop sensor for detecting electromagnetic field caused by partial discharges in simulated insulation system of inverter-fed rotating machine

Yuki Kudo\*, Naoyuki Yahara, Masato Fujimoto, Masahiro Kozako, Masayuki Hikita  
Kyushu Institute of Technology

E-mail : hikita@ele.kyutech.ac.jp

**Abstract**—This paper deals with development of small loop antenna sensors with 10 mm in diameter for detecting electromagnetic (EM) waves emitted by partial discharges in the insulation system of inverter-fed motors. Partial discharges (PD) were generated with a pair of crossed enamel wires under ac voltage at 10 kHz for examining various fundamental properties of the small loop sensors; i.e. the frequency response, the distance dependence from the PD source to the sensor. The sensitivity of the small loop sensor was also measured. As a result, it was found that the developed small loop antenna allows detection of EM waves over the frequency range up to 4 GHz and can detect PD current pulse with its peak magnitude as small as 12.6pC. It is also suggested that the array of the developed loop sensors can be applied for PD localization in practical rotating machines under the so-called repetitive voltage impulse. It was found that the developed loop sensor can be also applied to detect and locate the PD source.

**Keywords:** *small loop sensor, partial discharge, electromagnetic wave, insulation diagnosis, localization, rotating machine*

## I. INTRODUCTION

In recent years, power devices have advanced remarkably in that they are operated at higher frequency and higher voltage. These situations bring about more highly efficient power conversion and control. On the other hand, a new problem arise called inverter surge occurring in the inverter-fed motor insulation system. Various examinations have been made as countermeasure against the inverter surge problem, especially on the evaluation and the diagnosis of the insulation system under repetitive impulse voltage [1-3].

The authors study diagnosis of the inverter-fed motor insulation system by paying attention to partial discharge (PD) that is precursor phenomenon of dielectric breakdown [4]. We now investigate diagnosis of the insulation system in viewing PD location on the basis of time of flight principle by positioning multiple electromagnetic wave (EMW) detecting small sensors inside an inverter-fed motor. In this paper, small loop type electromagnetic sensor (loop sensor hereafter) for PD emitted EMW detection was fabricated. PD measurement was carried out for a winding model electrode so as to discuss fundamental properties of the developed sensors such as the distance dependence etc. An attempt is also made to localize PD in the formed coil (diamond shape coil) used for a high voltage motor. The possibility of the rotating machine insulation diagnosis application of the loop sensor was examined from these results.

## II. EXPERIMENTAL METHOD

Figure 1 shows the loop sensor that we developed. Loop pattern was made on the surface of a printed-circuit board. The terminal of the pattern was connected with SMA cable by solder using a receptacle.



Fig.1 Small loop type electromagnetic field sensor

Figure 2 shows experiment circuit and configuration of a test electrode with crossed enamel sample [5]. The crossed enamel sample is prepared in such a way that two enamel wires are crossed and touched each other at the center of the enamel ware. Commercially available enamel wire KMKED-20E (Hitachi Magnet Wire Corp, the conductor diameter: 0.724mm) was used. PD measurements were made with a digital oscilloscope (Tektronix, DPO7254, analog bandwidth 2.5GHz) and a spectrum analyzer (Agilent, E7405A, bandwidth 30Hz~26.5GHz). To measure PD, ac voltage of 780Vrms was applied to the crossed sample of 10kHz. Note that the magnitude of the voltage was 1.2 times larger than that of partial discharge inception voltage (PDIV). Subsequently, EMW caused by PD in the crossed electrode was detected with the developed loop sensor, and PD current was detected through the impedance matching circuit with the oscilloscope. Signal detected by the loop sensor was measured with the oscilloscope through a high-pass filter (Mini-Circuits, BHP-400+, bandwidth 395MHz~3200MHz). The above PD measurement was conducted both in an anechoic-room and a usual laboratory space. Frequency of PD emitted EMW detected by the loop sensor and a horn antenna (SCHWARZBECK, BBHA-9120A, bandwidth 750MHz~5GHz) in the crossed sample was compared using the spectrum analyzer. EM wave arising from noises and PD were measured for 3 minutes through 40dB amplifier (Techno Science Japan, MLA0120-A01-34). The loop sensor and the horn antenna were located at the distance  $D=5\text{cm}$  and  $100\text{cm}$  apart from the crossed point of the sample, respectively.

We obtained signal arrival time difference and each signal magnitude detected by the loop sensor as a function of the distance  $D$  between the sensor position and the cross point. Figure 3 shows the experiment circuit for PD location in a diamond coil. To cause PD in the diamond coil at an arbitrary position, a part of the diamond coil was grounded. PD emitted EMW signal was acquired with four loop sensors as shown in Figure 3 by applying 60Hz ac voltage 1kVrms which was 1.2 times higher than PDIV. PD location was made from both the magnitude of EMW signal and the difference in the arrival time of the signal.

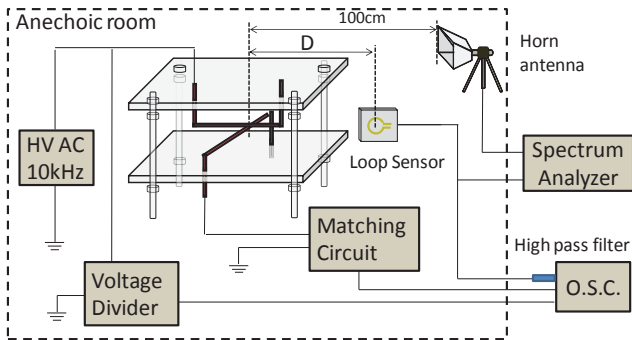


Fig.2 Configuration for measuring distance dependence of EMW detected with loop sensor

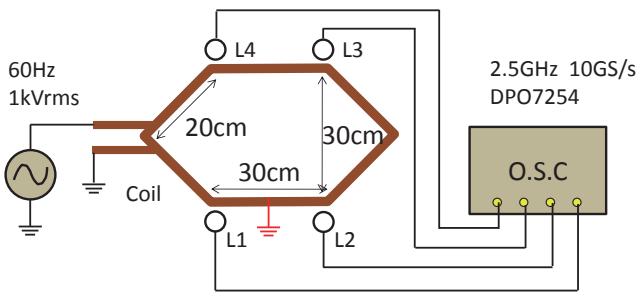


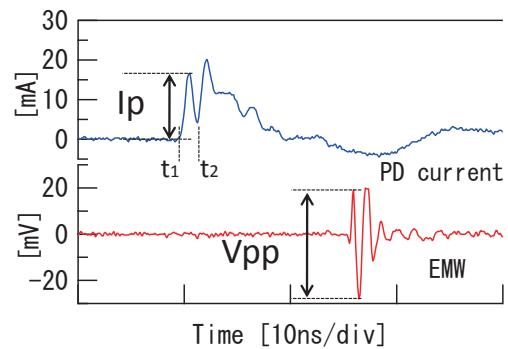
Fig.3 Measuring circuit for PD location in diamond coil

### III. RESULTS AND DISCUSSION

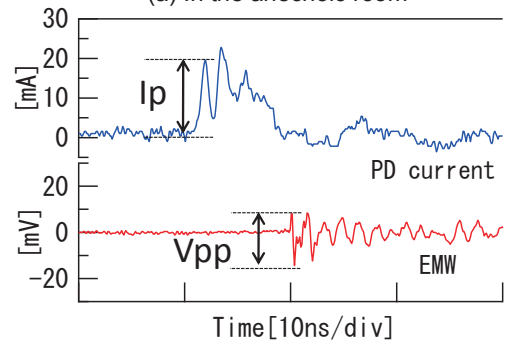
#### A. PD emitted EMW characteristics in crossed enamel sample

Figure 4 (a) and (b) show example of waveforms of EMW and current measured in the anechoic-room and the laboratory, respectively. It should be noticed in the figure that PD current waveform is composed of two or more pulses with 1.5ns interval. The phenomenon is attributed to reflection of the signal at the open-edge of the crossed enamelled wire. It is also seen that the waveform detected by the loop sensor is distorted by the reflection of EM wave from the base and the wall in the laboratory space. With the influence of the reflection considered, the peak value  $I_p$  of the first pulse of PD current and peak-to-peak value  $V_{pp}$  of EMW signal in the first cycle were used as the magnitude of detected PD signal. These values of  $I_p$  and  $V_{pp}$  were determined by averaging 30 data. Figure 5 shows thus obtained relation between PD current  $I_p$  and EMW signal  $V_{pp}$  detected by the loop sensor. It is evident in the anechoic-room measurement that linear relation between  $V_{pp}$  and  $I_p$  is obtained. On the other hand, in the

laboratory measurement experimentally obtained result has a discrepancy from the linear relation between  $V_{pp}$  and  $I_p$ . The discrepancy may arise from the waveform distortion caused by the superposition of the reflected wave. Figure 6 (a) and (b) show frequency spectrum of EMW emitted by PD occurring in the crossed sample measured with the horn antenna and the loop sensor in the anechoic-room, respectively. It is found from the figure (a) measured with the horn antenna that the frequency spectrum extends over 4GHz with 0.8GHz giving the maximum gain. Similarly, the frequency spectrum detected by the developed loop sensor extends over 4GHz with a slightly less gain than that for the horn antenna. It can be confirmed that the developed small loop sensor allows detection of EMW emitted by PD over a wide frequency band up to 4GHz.



(a) In the anechoic room



(b) In the laboratory

Fig.4 PD current and loop sensor signal waveform under different environment

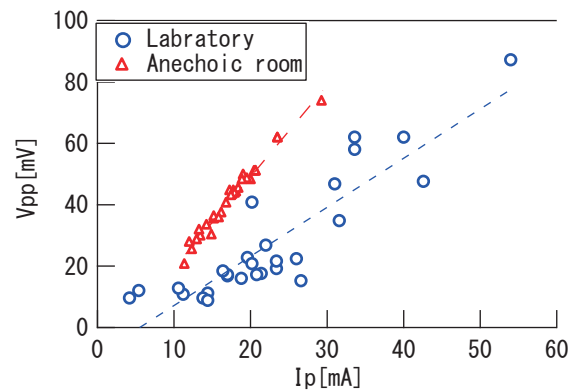


Fig.5 Correlation of PD current and signal strength

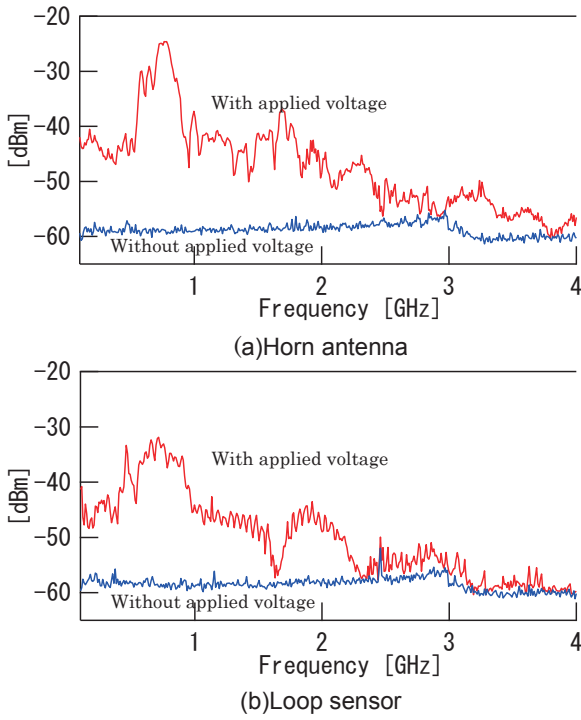


Fig.6 PD frequency response of cross electrode

### B. Distance dependence of PD signal in loop sensor

Figure 7 shows EM waveform detected with three loop sensors positioned at different distances. It is obvious in this figure that the magnitude  $V_{pp}$  decreases and the arrival time increases with increasing the distance from the signal source. Table 1 lists the measured difference in the time between three signals detected by three different loop sensors as well as the theoretically derived time difference when the velocity of EMW propagates at the speed of light. Note that the estimation error is  $\pm 100\text{ps}$  for used 10GHz sampling. It is shown in Table 1 that the signal arrival time difference obtained from the waveforms almost corresponds to the theoretical value. Figure 8 shows the distance dependence of  $V_{pp}$  measured by the loop sensor. Generally, when the characteristic impedance  $Z$  of EMW existing in a region differs much from that of free space  $Z_0=377\Omega$ , such EMW region is called near field. When  $Z$  of EMW in a region is almost equal to  $Z_0$ , the region is defined as far field. The boundary between the far field and the near field of EMW is given by the distance  $r$ .

$$r = \frac{\lambda}{2\pi} = \frac{c}{2\pi f} \quad (1)$$

Where  $\lambda$  is the wavelength,  $f$  is the frequency and  $c$  is the velocity of light. When discharge is assumed to be a minute current dipole, the magnetic field passing through a loop in the near field is given by the following equation [6].

$$H = \frac{Ie^{-jkr}}{4\pi} \left( \frac{1}{r^2} + \frac{jk}{r} \right) \sin\theta \quad (2)$$

Where,  $I$  is the current,  $l$  is the dipole length,  $k$  is the wavenumber, and  $\theta$  is the angle between current  $I$  and measurement point. Similarly, the magnetic field in the far field is given by the following equation.

$$H = \frac{jkIl}{4\pi} \frac{e^{-jkr}}{r} \sin\theta \quad (3)$$

Thus, the magnetic field passing through the loop is inversely proportional to the distance and the square of the distance in the far field and the near field, respectively.

Equation 1 shows that the boundary depends on the frequency of electromagnetic wave. Since, PD has a wide frequency component (Figure 6), the loop sensors located at different distances can acquire PD emitted EMW signal in both far field and near field. This consideration allows reasonable explanation for the result of Figure 8 showing the distance dependence of PD signal strength. Next, the sensitivity of the loop sensor is obtained from the relation between PD current  $I_p$  and  $V_{pp}$ . Figure 9 shows  $V_{pp}$  divided by the noise level when detected by the loop sensor as a function of PD apparent charge  $q$  which is defined by equation (4).

$$q = \int_{t_1}^{t_2} I_p dt \quad (4)$$

Note that the noise level of the loop sensor was 5mV on measurement. The sensitivity is obtained from the correlation curve of the PD current and the magnitude  $V_{pp}$  of EMW at a given distance  $D$ . Namely, the apparent charge  $q$  is assumed to be the integral of PD current waveform from the time  $t_1$  to  $t_2$  as shown in Figure (4). Table 2 lists the result of the sensitivity of the loop sensor derived from equation (4). As a result, it is found that the developed loop sensor has sensitivity of tens of pC for PD occurring from the crossed enamel sample.

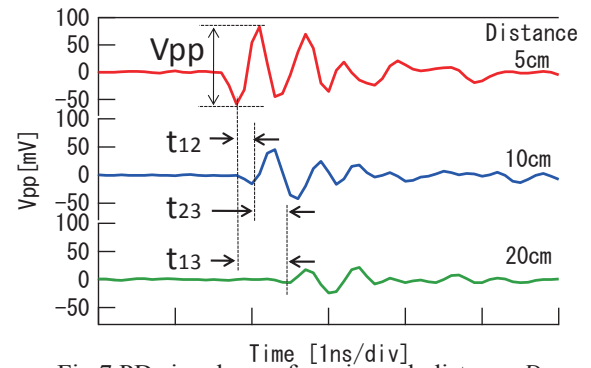

 Fig.7 PD signal waveform in each distance  $D$ 

Table.1 Time difference of arrival of PD signals

	Measurements	Theory
$t_{12}$	200 [ps]	166 [ps]
$t_{23}$	400 [ps]	333 [ps]
$t_{13}$	600 [ps]	500 [ps]

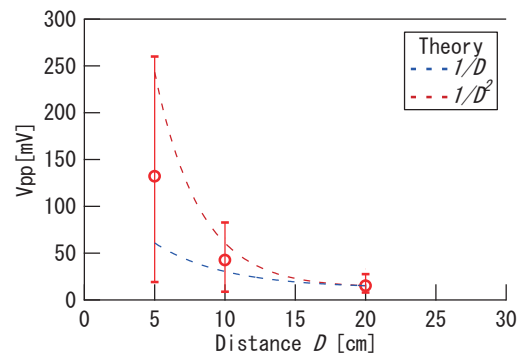


Fig.8 Distance dependence of PD signal strength

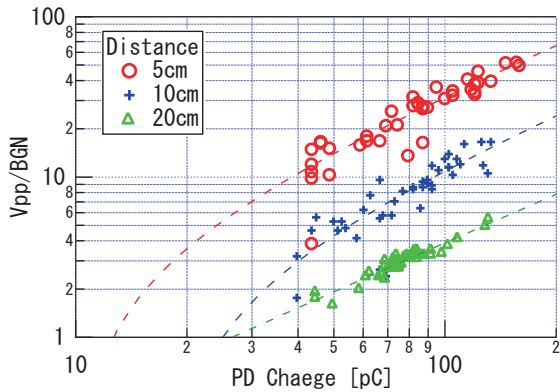


Fig.9 Sensitivity [mA] of loop sensor in each distance  $D$

Table.2 Sensitivity [pC] of loop sensor in each distance  $D$

Distance $D$	Sensitivity [pC]
5cm	12.6
10cm	25.6
20cm	26.6

C. PD location in the diamond coil

Figure 10 shows example of EM waveform detected with each loop sensor placed around the diamond coil. EMW with the peak magnitude  $V_{pp}$  exceeding 1.5 times of the noise level was taken as PD signal. Figure 11 show two typical examples of PD location made from the magnitude and the arrival time difference of EMW detected by each loop sensor. The origin of the horizontal axis of this figure represents the time when the loop sensor detected the signal first. In Figure 11 (a), loop sensors L1 and L2 located at the vicinity of the PD source acquire larger signal at the earliest timing, while loop sensors L3 and L4 acquire even weaker signal with 1.5ns delay. Similarly, it is confirmed from Figure 11 (b) that as the sensor position is apart from the PD source, the signal magnitude decreases and the arrival time increases. If it is assumed that the velocity of EMW propagating along the diamond coil is about 0.9 times of the speed of light, each loop sensor considered to acquire PD EMW signal is transmitting along winding conductor.

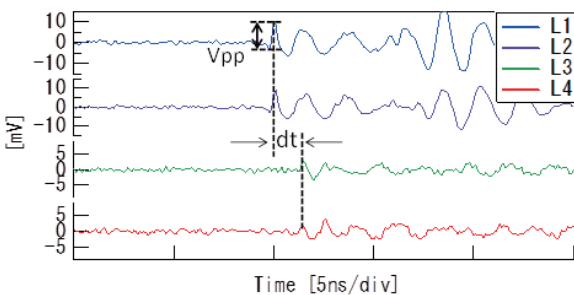


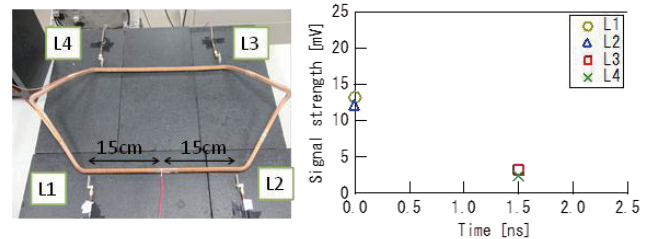
Fig.10 PD signal waveform of loop sensors in the diamond coil.

IV. CONCLUSION

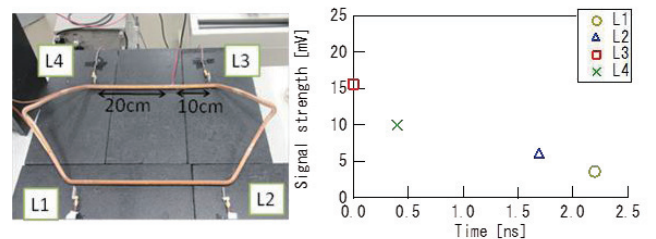
We now investigates diagnosis of the insulation system in viewing PD location on the basis of time of flight principle by positioning multi-small EMW detecting sensors inside an inverter-fed motor. In this paper, the possibility of the rotating machine insulation diagnosis application of the loop sensor was examined from the distance dependence of EMW detected by the loop sensor. It was confirmed that the developed loop sensor allows detection of EMW emitted by PD over a wide frequency band up to 4GHz. It is also found

that the distance dependence (signal magnitude and arrival time difference) measured by the loop sensor corresponds to the theory theoretical formula. It is also indicated that the developed loop sensors can be applied for PD localization in the diamond coil.

Further investigation is under way on the effect of the size of the loop sensor on the PD detection sensitivity. Moreover, PD measurement in a practical motor and construction of algorithm of PD location will be investigated.



(a) When the PD source is at the center of L1 and L2



(b) When the PD source is beside L3

Fig.11 Example of PD location in the diamond coil

REFERENCES

- [1] F. Perisse, D. Mercier, E. Lefevre, D. Roger "Robust Diagnostics of Stator Insulation Based on High Frequency Resonances Measurements" IEEE Transactions on Dielectrics and Electrical Insulation, Vol.16 No.5, 2009
- [2] S. H. Yi, D. H. Hwang, D. S. Kang "Research on PD Sensor Design for Stator Winding Diagnosis of Turbine Generators" The 8th International Power Engineering Conference, 2007
- [3] A. Kheirmand, M. Leijon, S. M. Gubanski "New Practices for Partial Discharge Detection and Localization in Large Rotating Machines" IEEE Transactions on Dielectrics and Electrical Insulation, Vol.10 No.6, 2003
- [4] M Fujimoto, K Yamaguchi, Y Kudo, M Kozako, M Hikita, Y Tsuda, Y Wakimoto, T Yoshimitsu "Partial Discharge Characteristics of Arrow Pair Sample with Simulated Cavity for Electrical Rotating Machine (III)" Japan Chapter of IEEE Society on Dielectrics and Electrical Insulation F-2, 2010
- [5] S Okada, K Fukunaga, K Yamaguchi, M Hikita "Relation of apparent charge, optical intensity, and partial discharge radiation electromagnetic wave in crossed sample under repetition impulse voltage" Joint Conference of Electrical and Electronics Engineers in Kyusyu 01-2A-08, 2007, (In Japanese)
- [6] M Asada, T Hirano, Electromagnetics, Baifukan, 2009 (In Japanese)